

Nitrogen in Oxides

Electrical Characterization and Computational Studies of
Defect Equilibria and Electronic Structure

Jonathan M. Polfus



Dissertation for the degree of Philosophiae Doctor

Department of Chemistry
Centre for Materials Science and Nanotechnology
Faculty of Mathematics and Natural Sciences
University of Oslo

August 2012

© Jonathan M. Polfus, 2012

*Series of dissertations submitted to the
Faculty of Mathematics and Natural Sciences, University of Oslo
No. 1248*

ISSN 1501-7710

All rights reserved. No part of this publication may be
reproduced or transmitted, in any form or by any means, without permission.

Cover: Inger Sandved Anfinsen.
Printed in Norway: AIT Oslo AS.

Produced in co-operation with Akademika publishing.
The thesis is produced by Akademika publishing merely in connection with the
thesis defence. Kindly direct all inquiries regarding the thesis to the copyright
holder or the unit which grants the doctorate.

Preface

This dissertation represents part of the requirements for the degree of Philosophiae Doctor (Ph.D) at the Faculty of Mathematics and Natural Sciences, University of Oslo. The doctoral scholarship has been part of the *Nitrogen in Oxides* project (#191346) funded by the Research Council of Norway through the FRINAT program. Computational resources were provided by the NOTUR project (The Norwegian Metacentre for Computational Sciences) under the project nn4604k. The work was conducted at the Group for Solid State Electrochemistry at the Department of Chemistry between September 2009 and September 2012 under the supervision of Associate Professor Reidar Haugsrød and Professor Truls Norby. The experimental work described in Paper II was conducted for my Master of Science degree prior to the Ph.D scholarship.

First of all I wish to thank my supervisors Reidar Haugsrød and Truls Norby. Your guidance, encouragement and positive involvement in my work has been highly appreciated. I would also like to thank Professor Isao Tanaka and Associate Professor Fumiyasu Oba at Kyoto University for their hospitality and fruitful collaboration during my stay in Japan.

Special thanks to Tor S. Bjørheim and Kazuaki Toyoura for many scientific discussions and good times during the past years. I would also like to acknowledge my project partner Charles H. Hervoches and my fellow students and colleagues at the Group for Solid State Electrochemistry for a social and comfortable working environment. I have particularly enjoyed sharing office with Ragnhild Hancke and Camilla K. Vigen. Finally I wish to thank my family and friends for support along the way.

Oslo, August 2012

Jonathan M. Polfus

Summary

The present work deals with the nitrogen related defect chemistry of wide band gap oxides and how nitrogen substitution may affect their functional properties through changes in defect equilibria and electronic structure. The primary objective has been to determine the type and charge state of various nitrogen defects and their concentration as a function of temperature and atmospheric conditions. The physical properties of these defects may be utilized to tailor functional properties related to e.g. ionic and electronic transport, photocatalytic properties and corrosion.

First principles calculations were employed to determine the equilibrium defect structure of a range of wide band gap oxides and to obtain insight into the atomistic and electronic structure of oxides containing various nitrogen defects. The considered oxides comprised MgO, CaO, SrO, Al₂O₃, In₂O₃, Sc₂O₃, Y₂O₃, La₂O₃, TiO₂, SnO₂, ZrO₂, BaZrO₃ and SrZrO₃. The defects considered were, in Kröger-Vink notation, N_O^q, NH_O^X, and (NH₂)_O[•] as well as V_O^{••} and OH_O[•]. The N_O^q acceptor level was found to be deep and the binding energy of NH_O^X with respect to N_O^l and OH_O[•] was found to be significantly negative, i.e. binding, in all of the investigated oxides. The defect structure of the oxides was found to be remarkably similar under reducing and nitriding conditions (1 bar N₂, 1 bar H₂ and 1 × 10⁻⁷ bar H₂O): NH_O^X predominates at low temperatures and [N_O^l] = 2[V_O^{••}] predominates at higher temperatures (>900 K for most of the oxides). In terms of electronic structure, N_O^l was found to introduce isolated N-2p states within the band gap, while the N-2p states of NH_O^X are shifted towards, or overlap with the VBM. Accordingly, NH_O^X may be more suitable than N_O^l for tuning the band gap of oxides.

Experimental investigation of RE₂O₃ (RE = Nd, Gd, Er, Y) and ZrO₂ specimens treated in NH₃ up to 1473 K corresponded well with the defect structure predicted computationally. In the case of Y₂O₃, the NH_O^X concentration was estimated to 7 × 10⁻³ mol fraction in a specimen quenched in NH₃ from 1473 K which was argued to be in reasonable agreement with the concentration predicted theoretically, 5 × 10⁻² mol fraction. Based on electrical conductivity measurements, it was established that dissolution of NH_O^X in NH₃ atmosphere had no significant effect on the electrical properties, as expected due to the effectively neutral charge of this species. However, as the nitriding atmosphere was replaced with an inert gas, a transient increase in conductivity of more than one order of magnitude was observed. This was interpreted as dissociation of the NH_O^X species followed by out-diffusion of hydrogen, leaving N_O^l which then must be charge compensated by other positive defects such as oxygen vacancies and electron holes, which can account for the increase in conductivity. This transient effect then represents a non-equilibrium process in which the out-diffusion of hydrogen, most probably as protons, is faster than that of nitrogen.

The defect chemistry of a Σ3 (111) grain boundary in BaZrO₃ was investigated by first

principles calculations and space-charge theory models. It was of particular interest to determine whether accumulation of N_O^{\prime} in the otherwise positive boundary core could suppress the space-charge potential by lowering the core charge. However, N_O^{\prime} exhibited a limited segregation tendency to the core due to a positive segregation energy of 0.08 eV. On the other hand, the segregation energy of protonic defects was significantly negative, -0.81, -0.58 and -1.36 eV for OH_O^{\bullet} , NH_O^{\times} and $(NH_2)_O^{\bullet}$, respectively. The concentration enhancement of nitrogen defects in the core was significant, and it was determined that N_O^{\prime} , NH_O^{\times} and $(NH_2)_O^{\bullet}$ can predominate the core in different temperature regimes but not suppress the unwanted space-charge effects.

The nitrogen and hydrogen related defect chemistry of mayenite, $Ca_{12}Al_{14}O_{33}$, was investigated due to its unique structure which can host rather unusual defect species. Results from first principles calculation suggest that nitrogen is primarily incorporated substitutionally on oxygen sites as NH_2^- and N^{3-} . The concentration of nitrogen was estimated to within the same order of magnitude by the computational methods and X-ray photoelectron spectroscopy (XPS) and gas phase mass spectrometry (GP-MS) of specimens quenched in NH_3 from 1223 K, yielding a stoichiometry close to $Ca_{12}Al_{14}O_{31.5}N_{0.5}:(NH_2)_{0.5}O_{0.5}$. Out-diffusion of nitrogen was found to occur around 973 K in Ar by XPS and GP-MS in accordance with previous reports. This process was accompanied by an abrupt increase in conductivity due to the lack of a sufficiently large source of oxygen in the surrounding atmosphere, so that the specimen was effectively reduced. Dissolution of hydride ions from H_2 in the reduced and highly conductive post- NH_3 state was substantiated.

Oxide nitrides and nitrides were evaluated as potential proton conducting ceramics by first principles calculation on $SrTaO_2N$ and $ThTaN_3$ perovskites. The level of proton incorporation was obtained from the thermodynamics of dissociative absorption of water and ammonia into anion vacancies in the acceptor doped materials. Protons were found to be significantly more stable associated with the nitride ions than the oxide ions in $SrTaO_2N$ and the proton position and bond length to the anions in both materials were mostly very similar to those in corresponding perovskite oxides such as $SrZrO_3$. In comparison to $SrZrO_3$, the concentration of protons was predicted to be significantly lower in $ThTaN_3$ and $SrTaO_2N$.

Finally, the defect chemistry of nitrogen in oxides was reviewed with particular emphasis on experimental and theoretical investigations relevant to the present work. Furthermore, the electronic structure and stability of a fully NH_O^{\times} substituted oxide nitride, $SrTa(NH)_2N$, was discussed.

Table of Contents

Preface	i
Summary	iii
1 Introduction	1
2 Methodology	3
2.1 Experimental	3
2.2 Computational	3
3 Papers	11
I Nitrogen defects in wide band gap oxides: defect equilibria and electronic structure from first principles calculations	13
II Nitrogen defects from NH ₃ in rare-earth sesquioxides and ZrO ₂	23
III Defect chemistry of a BaZrO ₃ Σ3 (111) grain boundary by first principles calculations and space-charge theory	29
IV Nitrogen and hydrogen defect equilibria in Ca ₁₂ Al ₁₄ O ₃₃ : a combined experimental and computational study	39
V Protons in perovskite nitrides and oxide nitrides: A first principles study of ThTa ₃ N and SrTaO ₂ N	49
VI The defect chemistry of nitrogen in oxides: A review of experimental and theoretical studies	55

Chapter 1

Introduction

Materials science is a corner stone of technology and has, as such, an immense impact on modern societies. Particularly, successful implementation of renewable energy sources relies on improved functional materials for use in for instance fuel cells, batteries and solar cells, and greenhouse gas emission from fossil fuels can be reduced by utilizing gas separation membranes. Furthermore, as functional materials are exceedingly utilized in devices within information technology, telecommunication and medicine, they allow for improved standards of living. In this respect, it is important to realize that state-of-the-art technologies are relevant for developing countries since material and production costs as well as power consumption often can be kept to a minimum for solid-state components; examples include photocatalytic purification of water¹, polymer based solar cells for off-grid power supply² and light emitting diodes (LED) for increased access to clean, safe and affordable lighting.³

In order to improve the functional properties of materials, fundamental understanding of their physical origin is necessary. Functional properties of crystalline solids are to a large extent determined by the type and concentration of defects in the material; defect induced properties can be related to for instance electronic and ionic transport, catalysis, magnetism, optical phenomena and corrosion. Metal oxides, which are the primary focus in this thesis, are central for many applications due to their many extraordinary and useful properties as well as stability and availability. Traditionally, the defect chemistry of oxides has been tailored through the addition of aliovalent cations or treatment under oxidizing or reducing conditions to inflict oxygen non-stoichiometry. In the present work, the nitrogen related defect chemistry of oxides is investigated in order to evaluate the potential of nitrogen as an additional variable for tailoring the functional properties of oxides.

First principles computational methods have been utilized to investigate the nitrogen related defect chemistry of wide band gap oxides, e.g., Y_2O_3 , ZrO_2 , TiO_2 and SrZrO_3 , with particular emphasis on the interaction between nitrogen and protonic defects. Such calculations provide detailed insight into the atomistic and electronic structure of nitrogen containing oxides and allow for efficient study of many compounds. Experimental studies have been performed on similar oxides in order to verify the computational findings and to elucidate the kinetic aspects of nitrogen incorporation. Specifically, electrical conductivity measurements were utilized to probe the defect chemical processes taking place while the oxide specimens were equilibrated at elevated temperatures with ammonia atmospheres as the nitriding agent. The electrical characterization was supported by other techniques such as X-ray diffraction (XRD) to ensure

that the crystallographic structure remained unchanged, X-ray photoelectron spectroscopy (XPS) for semi-quantitative analysis of nitrogen in the oxide structure, and gas phase mass spectrometry (GP-MS) for semi-quantitative analysis of nitrogen and hydrogen diffusing out of the NH₃ treated specimens.

As a mineral with a complex cage structure and some rather unusual properties, mayenite (Ca₁₂Al₁₄O₃₃) represents a unique structural and chemical environment which has served as a model compound to further explore how nitrogen can behave in oxide materials. Association between nitrogen and protons was of particular interest also in this material and conductivity measurements were employed to elucidate on non-equilibrium processes associated with the nitrogen and hydrogen related defect chemistry.

The grain boundaries in polycrystalline materials represent another characteristic environment for defects and they can significantly affect the functional properties of the material. Particularly, the proton transport properties of polycrystalline acceptor substituted BaZrO₃ suffers from high grain boundary resistivity due to the depletion of protons in the space-charge regions. First principles calculations were performed for a symmetric tilt boundary in BaZrO₃ in order to obtain detailed insight into the defect chemistry of the core-space-charge system with respect to external variables such as temperature and atmospheric conditions. Especially, it was investigated whether nitrogen defects could improve the proton conducting properties of such oxides by suppressing disadvantageous space-charge effects.

Finally, mixed oxide nitride and nitride phases within the perovskite structure, SrTaO₂N and ThTa₃N, respectively, have been evaluated as proton conducting ceramics by first principles calculation of the thermodynamics of proton incorporation according to dissociative absorption of H₂O and NH₃. Furthermore, aspects related to materials design within the perovskite oxide and nitride systems are discussed.

This thesis is based on six manuscripts concerning the nitrogen and hydrogen related defect chemistry of oxides, oxide nitrides and nitrides. Prior to the manuscripts, an introductory part on the methodology will be given; the experimental part should be considered supplementary to what is described in the manuscripts while the computational part is meant as a short introduction to the underlying principles of density functional theory (DFT), as well as some aspects related to the practical implementation and accuracy of this methodology in material science and defect chemistry. In the last part of the thesis, relevant literature and a discussion covering the manuscripts will be provided in the form of a review article.

Chapter 2

Methodology

2.1 Experimental

Non-oxidizing conditions is a prerequisite for dissolution of substitutional nitrogen into an oxide due to the lower thermodynamic stability of nitrides relative to the corresponding oxides.⁴ Furthermore, due to the high stability of the N₂ molecule and exceptional strength of the N≡N bond ($\Delta H_{\text{diss}}^\circ = 946 \text{ kJ mol}^{-1}$), the direct reaction between N₂ and oxides has not proven to be effective.⁵ On the other hand, ammonia (NH₃) is a widely used nitrogen source for incorporation of nitrogen into oxides and preparation of oxide nitrides and nitrides from oxide precursors.⁴⁻⁸ At typical reaction temperatures, $600 \text{ }^\circ\text{C} < T < 1200 \text{ }^\circ\text{C}$, NH₃ will decompose into inactive N₂ and H₂ and thermal ammonolysis must therefore be carried out under non-equilibrium conditions by keeping a high NH₃ flow rate in order for reactive nitriding species to be present in the high temperature gas mixture. A continuous exchange of the atmosphere in the reaction chamber also ensures removal of oxidizing species such as H₂O originating from reaction product and leakages. A gas mixer unit, illustrated in Fig. 1, was utilized to obtain controlled atmospheres during electrical characterization. The mineral oil bubblers ensure overpressure control and excess gas relief. The gas outputs from the measurement cell and from M1-M4 were bubbled through lactic acid (not shown in the figure) to neutralize excess NH₃. Lactic acid is a liquid which forms a non-harmful liquid salt, ammonium lactate, upon reaction with NH₃, thereby keeping the ammonia trap from clogging at all times.

2.2 Computational

Introduction

The mutually interacting electrons and nuclei that define a material represent a many-body system for which an exact quantum mechanical treatment is generally not possible; approximations are necessary. For the so-called first principles or *ab initio* methods, such as DFT, these approximations comply with fundamental quantum mechanical principles and do not involve empirical models. In this respect, the Born-Oppenheimer approximation,⁹ which separates the electronic and nuclear degrees of freedom, can be applied on the basis that the dynamics of nuclei are much slower than the dynamics of electrons. The foundation for DFT

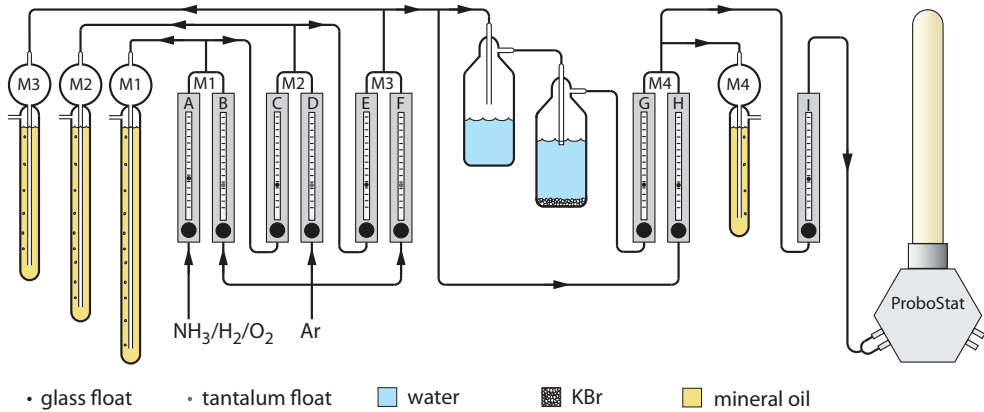


Figure 1: Schematic of the gas mixer unit and measurement cell (NorECs, Norway) utilized for electrical characterization in controlled atmospheres at approximately atmospheric pressure.

was laid through the Hohenberg-Kohn¹⁰ theorems which demonstrate that all physical ground state properties of an electronic system are uniquely determined by the electron density, and that the ground state energy is only obtained with the true ground state density. As such, the challenge of obtaining the wave function for a system of N electrons with a total of $3N$ spatial variables is reduced to obtaining the electron density which depends on only 3 spatial variables. A practical scheme to describe the form of the hitherto unknown functional necessary to obtain the ground state energy from the electron density was suggested by Kohn and Sham.¹¹ They introduced a reference system of non-interacting one-electron wave functions for which the major part of the kinetic energy of the electrons could be calculated exactly. The remaining part of the kinetic energy and the non-classical parts of the potential energy, i.e., related to electron self interaction correction, exchange and correlation, remains unknown and must be approximated.

The first approximation to the exchange-correlation functional, the local density approximation (LDA), was proposed in the original paper by Kohn and Sham.¹¹ Within LDA, the exchange-correlation energy per electron in a given point is assumed to be the same as that of a homogeneous electron gas with the same density (for which the exchange energy is known exactly¹² and the correlation energy can be calculated numerically with high accuracy¹³). Despite its basis in a hypothetical uniform electron gas, LDA performs quite well for many crystalline systems and is still used today. The generalized gradient approximation¹⁴ (GGA) is a natural improvement over LDA by also taking into account the variation in the electron density at a given point. GGA exists as a variety of parameterizations, e.g., PBE¹⁵, PW91^{16,17} and BLYP^{18,19}.

In the last decades, density functional theory based methods have proven their relevance for materials science due to their capable physical description of solids and computational efficiency. The bulk properties of solids, i.e., lattice constants, bulk moduli and cohesive energies, are generally well reproduced.²⁰ In this respect, GGA is in many cases a significant improvement over LDA especially for molecules and magnetic systems.²¹ These functionals,

however, suffer from a severe underestimation of band gaps. This problem has been addressed by developing computationally efficient hybrid functionals which mix DFT exchange with exact non-local Hartree-Fock exchange. In addition to improved bulk properties, hybrid functionals such as PBE0²² and HSE²³ offer significantly improved band gaps for semiconductors and insulators including oxides, nitrides and sulphides.^{24,25}

In contrast to first principles methods, classical potential based methods are not always suitable for defect calculations involving non-stoichiometry or extrinsic defects due to the lack of experimental references necessary to optimize the empirical parameters for such defective systems. On the other hand, classical potential based methods can be superior for dealing with disordered systems due to the implementation of partial occupancy and possibility for computing large supercells. However, although the crystallography of such systems may be well described, energetics and thermodynamic data are less reliable.

Practical implementation and accuracy

The periodicity of crystalline solids can be exploited by implementing periodic boundary conditions such that only the unit cell needs to be considered explicitly. Accordingly, the electronic charge density can be efficiently described through superposition of plane waves. On the basis that core electrons can be considered inert, pseudopotentials are implemented to represent the nucleus and core electrons of an atom (frozen core approximation), and only the valence electrons are considered in the calculation. The cut-off energy, i.e., upper limit frequency of the plane waves, can thereby be reduced to improve the computational cost due to the large number of plane waves necessary to accurately describe the rapidly oscillating wave functions close to the nuclei. The projector augmented wave (PAW) method²⁶ delivers improved accuracy by accounting for the nodal features of the valence orbitals and ensuring orthogonality between valence and core wave functions. Finally, since the electronic wave functions at k -points close to each other within the Brillouin zone (i.e. primitive cell in reciprocal space) are almost identical, the system can be evaluated at a finite number of k -points.

In practice, the input parameters for a DFT calculation of a material are simply the elemental composition and (initial) atomic positions. The electronic charge density is calculated within the Born-Oppenheimer approximation and the total energy and forces acting on all ions are obtained. Consequently, the atomistic structure can be optimized in an iterative procedure to a required accuracy with respect to total energy and forces on the atoms. For solids with point defects (which lack perfect periodicity) supercells can be employed to approximate an isolated system by minimizing interactions between the periodic images of the defect. Various defect charge states can be considered by adjusting the total number of electrons in the system as long as the intended defect charge state represents the ground state configuration so that the excess electrons/holes actually are associated with the defect. The spurious interaction between charged defects and the uniform background charge applied to charged cells can be corrected by aligning the electrostatic potential in a bulk-like area of the defective cell to the perfect cell.²⁷ As such, the magnitude of the error introduced by using the supercell method can be kept to a minimum, e.g., the difference in defect formation energy between 80 and 640 atom Y_2O_3 supercells was within 5 meV for the effectively neutral imide, $\text{NH}_\text{O}^\times$, and within 73 meV for singly charged hydroxide, $\text{OH}_\text{O}^\bullet$ (additional details in Paper I).

The free energy of formation of a defect can be calculated from the total energy difference between a defective and perfect cell and a set of chemical potentials, μ ,

$$\Delta G_{\text{defect}}^f(T, p) = E_{\text{defect}}^{\text{tot}} - E_{\text{perfect}}^{\text{tot}} + \sum_i \Delta n_i \mu_i(T, p) + q\mu_e \quad (1)$$

where Δn_i is the difference in the number of constituent atoms of type i between these cells and q is the effective charge state of the defect.²⁸ The atomic chemical potentials, $\mu_i(T, p)$, define the environmental conditions. The Fermi level or chemical potential of electrons, μ_e , can be defined only when equilibrium is established and therefore depends on the concentration and charge of all defects. Thus, in order to determine the general behavior of one or more defects in a material, the Fermi level is considered a variable and the defect formation energy can be evaluated as a function of it, as shown in Fig. 2 for N_O^q and V_O^q . The equilibrium Fermi level, μ_e^{eq} , can be determined for a set of conditions (T , μ_O and μ_N) by imposing the electroneutrality condition, e.g., $[N_O] = 2[V_O^{+}] + [V_O^{-}]$. As such, a physical description of the defect structure of the material can be obtained from the defect diagram. The thermodynamic transition levels between defect charge states, denoted ε in the figure, are independent of environmental conditions and other defects in the system. The absolute position of these defect levels relative to the band edges are obviously subject to relatively large variations depending on the approach used for the exchange-correlation functional due to the band gap problem.^{29,30}

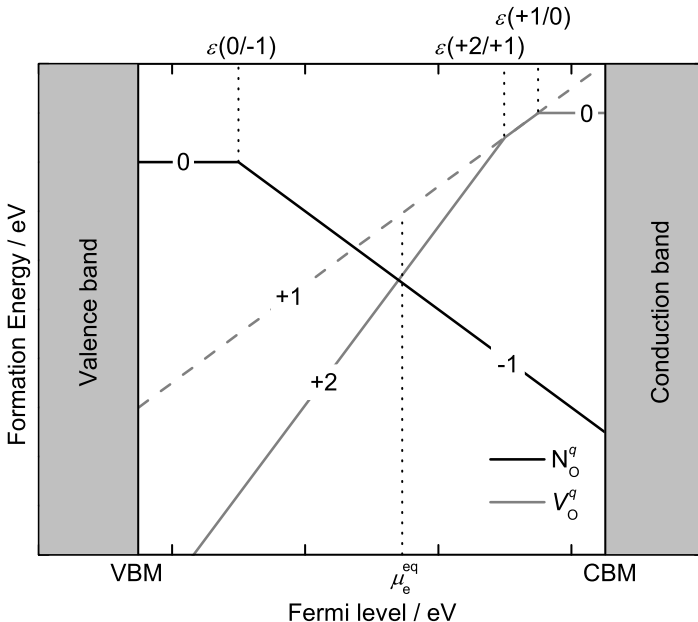


Figure 2: Schematic diagram of the formation energy of N_O^q and V_O^q as a function of the Fermi level which varies between the valence band maximum (VBM) and conduction band minimum (CBM). The slopes are indicated with the defect charge state, q .

Fortunately, the position of the transition levels relative to each other has been shown to be similar between GGA and hybrid functional calculations.^{31,32} For the wide band gap materials considered in this work, it is also reasonable to assume that defects predominately exist in their fully ionized charge states and accurate transition levels are therefore not crucial for obtaining the correct equilibrium defect structure given that the defect formation energies are adequate. In this respect, the difference in defect formation energies from GGA and HSE type calculations was within 6 % for N_O^I and $\text{OH}_\text{O}^\bullet$ in 80 atom Y_2O_3 cells at the equilibrium Fermi level (Paper I), and within 10 % for the hydration enthalpy of mayenite (Paper IV). The hydration enthalpy of SrZrO_3 exhibited a larger difference of approximately 20 % between GGA and HSE based calculations (Paper I and V, respectively). This may partly be attributed to the rather large difference in supercell size, 360 and 80 atoms for GGA and HSE, respectively. The significant discrepancies in the reaction enthalpies (e.g. hydration enthalpy) with the LDA based hybrid functional noted in Paper V may partly be attributed to the 0.49 eV error in the binding energy of the H_2O molecule with LDA compared to the 0.03 eV error with GGA.³³

References

- 1 M. Shannon, P. Bohn, M. Elimelech, J. Georgiadis, B. Marinas, and A. Mayes, *Nature*, 2008, **452**, 301–310.
- 2 F. Krebs, T. Nielsen, J. Fyenbo, M. Wadstrøm, and M. Pedersen, *Energy. Environ. Sci.*, 2010, **3**, 512–525.
- 3 <http://www.lightingafrica.org/>, 2007.
- 4 S. H. Elder, F. J. Disalvo, L. Topor, and A. Navrotsky, *Chem. Mater.*, 1993, **5**, 1545–1553.
- 5 R. Marchand, Y. Laurent, J. Guyader, P. Lharidon, and P. Verdier, *J. Eur. Cer. Soc.*, 1991, **8**, 197–213.
- 6 F. Tessier and R. Marchand, *J. Solid State Chem.*, 2003, **171**, 143–151.
- 7 M. T. Weller, R. W. Hughes, J. Rooke, C. S. Knee, and J. Reading, *Dalton Trans.*, 2004, **19**, 3032–3041.
- 8 S. G. Ebbinghaus, H. P. Abicht, R. Dronskowski, T. Muller, A. Reller, and A. Weidenkaff, *Prog. Solid State Ch.*, 2009, **37**, 173–205.
- 9 M. Born and R. Oppenheimer, *Ann. Phys.*, 1927, **84**, 0457–0484.
- 10 P. Hohenberg and W. Kohn, *Phys. Rev. B*, 1964, **136**, 864–871.
- 11 W. Kohn and L. J. Sham, *Phys. Rev.*, 1965, **140**, 1133–1138.
- 12 W. Koch and M. Holthausen, *A chemist's guide to density functional theory*, Vol. 2, Wiley Online Library, 2001.
- 13 D. M. Ceperley and B. J. Alder, *Phys. Rev. Lett.*, 1980, **45**, 566–569.
- 14 D. C. Langreth and M. J. Mehl, *Phys. Rev. B*, 1983, **28**, 1809–1834.
- 15 J. P. Perdew, K. Burke, and M. Ernzerhof, *Phys. Rev. Lett.*, 1996, **77**, 3865–3868.
- 16 Y. Wang and J. P. Perdew, *Phys. Rev. B*, 1991, **44**, 13298–13307.
- 17 J. P. Perdew and Y. Wang, *Phys. Rev. B*, 1992, **45**, 13244–13249.
- 18 A. D. Becke, *Phys. Rev. A*, 1988, **38**, 3098–3100.

- 19 C. T. Lee, W. T. Yang, and R. G. Parr, *Phys. Rev. B*, 1988, **37**, 785–789.
- 20 V. N. Staroverov, G. E. Scuseria, J. Tao, and J. P. Perdew, *Phys. Rev. B*, 2004, **69**, 075102–11.
- 21 J. Hafner, *J. Comput. Chem.*, 2008, **29**, 2044–2078.
- 22 C. Adamo and V. Barone, *J. Chem. Phys.*, 1999, **110**, 6158–6170.
- 23 J. Heyd, G. E. Scuseria, and M. Ernzerhof, *J. Chem. Phys.*, 2003, **118**, 8207–8215.
- 24 J. Heyd, J. E. Peralta, G. E. Scuseria, and R. L. Martin, *J. Chem. Phys.*, 2005, **123**, 174101–8.
- 25 J. Paier, M. Marsman, K. Hummer, G. Kresse, I. C. Gerber, and J. G. Angyan, *J. Chem. Phys.*, 2006, **124**, 154709–13.
- 26 P. E. Blöchl, *Phys. Rev. B*, 1994, **50**, 17953–17979.
- 27 T. Mattila and A. Zunger, *Phys. Rev. B*, 1998, **58**, 1367–1373.
- 28 S. B. Zhang and J. E. Northrup, *Phys. Rev. Lett.*, 1991, **67**, 2339–2342.
- 29 F. Oba, M. Choi, A. Togo, and I. Tanaka, *Sci. Technol. Adv. Mater.*, 2011, **12**, 034302–14.
- 30 N. D. M. Hine, K. Frensch, W. M. C. Foulkes, and M. W. Finnis, *Phys. Rev. B*, 2009, **79**, 024112–13.
- 31 A. Alkauskas, P. Broqvist, and A. Pasquarello, *Phys. Status Solidi B*, 2011, **248**, 775–789.
- 32 A. Alkauskas and A. Pasquarello, *Phys. Rev. B*, 2011, **84**, 125206–11.
- 33 D. C. Patton, D. V. Porezag, and M. R. Pederson, Mar , 1997, **55**, 7454–7459.

Chapter 3

Papers

I Nitrogen defects in wide band gap oxides: defect equilibria and electronic structure from first principles calculations

J. M. Polfus, T. S. Bjørheim, T. Norby and R. Haugsrud
Phys. Chem. Chem. Phys., 2012, **40**, 11808–11815

II Nitrogen defects from NH₃ in rare-earth sesquioxides and ZrO₂

J. M. Polfus, T. Norby and R. Haugsrud
Dalton. Trans., 2011, **40**, 132-135

III Defect chemistry of a BaZrO₃ $\Sigma 3$ (111) grain boundary by first principles calculations and space-charge theory

J. M. Polfus, K. Toyoura, F. Oba, I. Tanaka and R. Haugsrud
Phys. Chem. Chem. Phys., 2012, **14**, 12339–12346

IV Nitrogen and hydrogen defect equilibria in Ca₁₂Al₁₄O₃₃: a combined experimental and computational study

J. M. Polfus, K. Toyoura, C. H. Hervoches, M. F. Sunding, I. Tanaka and R. Haugsrud
J. Mater. Chem., 2012, **22**, 15828-15835

V Protons in perovskite nitrides and oxide nitrides: A first principles study of ThTaN₃ and SrTaO₂N

J. M. Polfus and R. Haugsrud
Solid State Commun., 2012, **152**, 1921-1923

VI The defect chemistry of nitrogen in oxides: A review of experimental and theoretical studies

J. M. Polfus, T. Norby and R. Haugsrud
J. Solid State Chem., 2013, **198**, 65-76

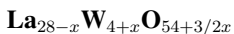
Additional contributions during the project period

- Complete structural model for lanthanum tungstate: a chemically stable high temperature proton conductor by means of intrinsic defects**

A. Magrasó, J. M. Polfus, C. Frontera, J. Canales-Vázquez, L. Kalland, C. H. Hervoche, S. Erdal, R. Hancke, M. S. Islam, T. Norby and R. Haugsrud

J. Mater. Chem., 2012, **22**, 1762-1764

- Defect structure and its nomenclature for mixed conducting lanthanum tungstates**



S. Erdal , L. Kalland, R. Hancke, J. M. Polfus, R. Haugsrud, T. Norby and A. Magrasó

Int. J. Hydrogen. Energ., 2012, **37**, 8051–8055

Nitrogen defects in wide band gap oxides: defect equilibria and electronic structure from first principles calculations

J. M. Polfus, T. S. Bjørheim, T. Norby and R. Haugsrud
Phys. Chem. Chem. Phys., 2012, **40**, 11808–11815

I

Nitrogen defects from NH₃ in rare-earth sesquioxides and ZrO₂

J. M. Polfus, T. Norby and R. Haugsrud
Dalton. Trans., 2011, **40**, 132-135



Defect chemistry of a BaZrO₃ $\Sigma 3$ (111) grain boundary by first principles calculations and space-charge theory

J. M. Polfus, K. Toyoura, F. Oba, I. Tanaka and R. Haugsrud
Phys. Chem. Chem. Phys., 2012, **14**, 12339–12346



Nitrogen and hydrogen defect equilibria in $\text{Ca}_{12}\text{Al}_{14}\text{O}_{33}$: a combined experimental and computational study

J.M. Polfus, K. Toyoura, C. H. Hervoches, M. F. Sunding, I. Tanaka and R. Haugsrud
J. Mater. Chem., 2012, **22**, 15828-15835

IV

Protons in perovskite nitrides and oxide nitrides: A first principles study of ThTa₃N and SrTaO₂N

J. M. Polfus and R. Haugsrud
Solid State Commun., 2012, **152**, 1921-1923



The defect chemistry of nitrogen in oxides: A review of experimental and theoretical studies

J. M. Polfus, T. Norby and R. Haugsrud
J. Solid State Chem., 2013, **198**, 65-76

VI

